Surface interaction of H_2O and O_2 on the ternary $Fe_{1-x}X_xAl$ metal alloy doped with Ru and Pd

Christine Mkhonto[1*], *Ndanduleni* Lethole[2], *Phuti* Ngoepe[1], and *Hasani* Chauke[1]

[1]Department of Physics and Geology, University of Limpopo, South Africa, Sovenga 0727

[2]Department of Computational Sciences, University of Fort Hare, Alice 5700, South Africa.

Abstract. Surface interaction is one of the most frequently utilized computational techniques for atomistic simulation and describing point defects in solid-state materials. The surface energy (energy of pure system)/or surface free energy (energy of the system with adsorbent) quantifies the disruption of intermolecular bonds when a surface is adsorbed on the ternary adsorbate $Fe_{1-x}X_xAl$. Typical surface properties such as adsorption, adhesion, weather resistance, corrosion resistance, and chemical resistance contribute to determining the stability of materials. The current study has explored the surface adsorption of H_2O and O_2 on the $Fe_{1-x}X_xAl$ ternary system to address the challenge of corrosion and oxidation effects. In particular, the surface interaction is investigated to cleave surface models by observing point defects of terminations to determine the bonding strength that can resist the oxidation process. The E_{ads}/H_2O showed higher energies compared to those of O_2, which implies that E_{ads}/O_2 is more stable with the lowest energies compared to those of H_2O.

1 Introduction

Surface interaction has allowed a broader spectrum to investigate and mitigate the challenges of oxidation for the development of solid-state materials, leading to improved component coating in stainless-steel and cost-effective production. Reactions on types of coating on the surfaces have been conducted by Fones and Hatton using computer simulations [1]. Their equilibrium structures (Wulff shape) were based on the Wulff cluster model. This model was proved preliminarily by calculating the concentration trend of Al/Fe atoms on both Al-terminated and Fe-terminated surfaces, and by simulating the mo`st stable layer adsorbed on these two surfaces. It was reported that environmental moisture-induced and temperature are leading causes of low tensile ductility and brittle cleavage fracture on the Fe-rich FeAl alloy. This results in deformation, fracture on the design of the β2 iron aluminide-based alloy, and poor yield-strength anomaly at intermediate temperature. However, possible cracks can be observed on the surface of the system if the surface yields low free surface energy contributing to fracture effects. Thus, there is still a need to explore the corrosion and oxidation behavior in order to increase adhesion, and capacity to tolerate creep resistance [2,

* Corresponding author: chresimkhonto@gmail.com

3]. In general, iron-aluminides are reported to show a major embrittlement mechanism at room temperature, resulting in a loss of cohesive strength at their interfaces [4].

On the other hand, intermetallic alloys exhibit unique surface properties, including high hardness, good wear and corrosion resistance, and the ability to form adherent surface oxides, making them suitable for applications for high-temperature structural components and coatings [5]. In order to understand the behaviour and interaction of the intermetallic, various surface terminations are considered. This is done by cleaving the most stable slab model, which will allow doping on the surface and adsorption. This provides valuable insight into the binding capacity, bonding strength and adhesion abilities, resulting in a reduction to surface oxidation. However, the strength of the material can be negatively influenced by environmental effects such as hazardous chemicals in the atmosphere, moisture, and heat, which may have the ability to deteriorate the mechanical properties. Mkhonto *et al.* A molecular dynamics study of $Fe_{50-X}M_XAl_{50}$ ternary alloy (M=Ag, Pt, Pd) in 2020, the intermetallic studies on the mechanical and dynamical properties of $Fe_{1-X}XxAl$ (X = Pt and Ru) Alloys, in 2022, the effect of alloying on β2-ordered FeAl with Pd and Ir for high-temperature application and ductility enhancement in 2023. This is to determine the effect of ternary alloying under various conditions to enhance the stability of iron aluminides [6, 7, 8]

It is crucial to consider factors affecting adhesion, durability, creep resistance, oxidation and ductility of the surface when exposed to various conditions for specific tailored applications in automotive parts, turbines, in particular, in aerospace infrastructures. The aluminides have remarkably become the most applied coating method in protective coatings because they possess excellent high-temperature corrosion resistance [9]. Maintaining aluminium content is favorable, and the adhesion scale to the substrate is a protective barrier, guaranteeing intermetallic alloys that are corrosion resistant [10, 11]. This study demonstrated that doping the pristine FeAl with Ru and Pd greatly improved its surface stability. Determining the surface interaction of H_2O and O_2 demonstrated the impact it has on the $F_{1-X}X_XAl$ ternary system after improving the stability of the system through adsorption a third metal on the pristine FeAl alloys.

2 Methodology

Computational modelling techniques such as VASP and CASTEP were employed to determine the surface stability of $Fe_{1-X}Ru/Pd_XAl$ systems. We have employed the first-principles DFT [12] method to determine the surface adsorption and bond strength of the ternary $F_{1-X}X_XAl$ system. The Perdew-Berke-Ernzerhof (PBE) [13] functional and generalized gradient approximation (GGA) [14] for estimating calculations were employed. Moreover, a plane-wave pseudopotential functional [15] with a cut-off energy of 270 eV was sufficient to allow the systems to converge. METADISE code [16], was used to cleave the conventional (110) surface plane of the pristine FeAl system. VESTA-win64 was also used to visualize crystal structures and three-dimensional data, including the volumetric data and crystal morphologies of the $F_{1-X}X_XAl$ system [17]. This is followed by cleaving slab models on the (110) surface plane in order to identify the suitable slab with the lowest surface energy for the design of ternary $Fe_{1-X}X_XAl$ systems by adsorbing a third element Ru and Pd to enhance surface stability which will be identified as surface free energy. Further calculations were done by determining the interaction of H_2O and O_2 on the ternary $F_{1-X}X_XAl$ system.

3 Results and discussion

3.1 H_2O interaction on $Fe_{1-X}Y_XAl$ system

In this section, we have carried out density functional theory calculations with long-range dispersion corrections to investigate the interaction of H_2O and O_2 on the most stable $Fe_{1-X}X_XAl$ (110) surfaces. This is done in order to determine the surface energies of the most stable site with different concentrations of X element. Ru and Pd are both platinum group metals with diverse properties and applications. Herein, Ru is a chosen adsorbent due to its hard, high boiling and melting point and does not tarnish at room temperature. Where else Pd is malleable and ductile. These adsorbents have the potential to enhance durability, increase oxidation and corrosion resistance of the pristine FeAl system. Thus, the introduction of H_2O and O_2 adsorption is to observe the effect as these materials will be exposed to various environmental conditions.

Figure 1 to Figure 2 illustrate adsorption of H_2O on the ternary $Fe_{1-X}Ru_XAl$ and $Fe_{1-X}Pd_XAl$ systems, respectively. The pristine FeAl alloy is a potential structural material especially when adsorbed with Ru/Pd adsorbents to enhance the strength and surface stability. Therein, there is a need to observe the interaction of H_2O on the $Fe_{1-X}Ru_XAl$ and $Fe_{1-X}Pd_XAl$ systems. This reaction has been known to have a negative effect on surface properties. These models were chosen due usage of METADISE code which cleaves slab models with zero dipole moment, that is, symmetrical shape, causing the bond of dipoles and in turn improving their physical properties, such as boiling point.

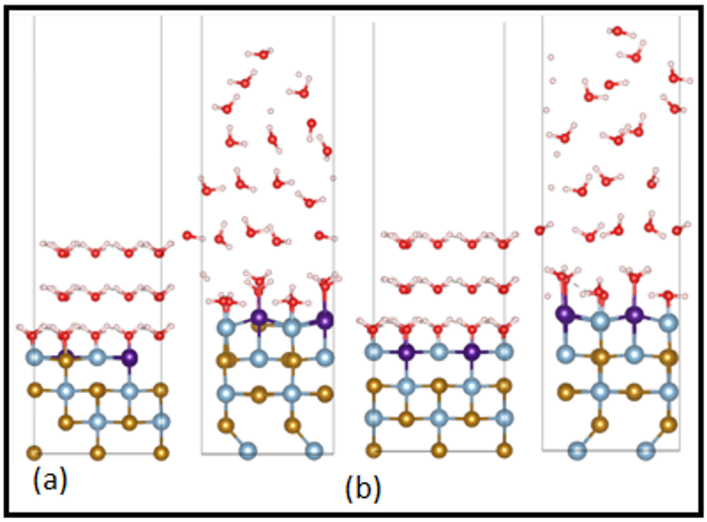

Fig. 1. Adsorption of H_2O on ternary $Fe_{1-X}X_XAl$ on (110) surface; brown- Fe, light blue- Al, dark blue representing the adsorbent Ru.

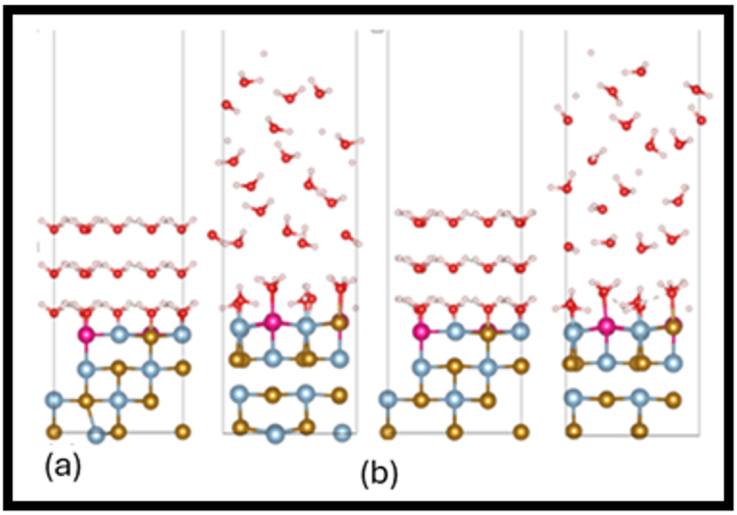

Fig. 2. Adsorption of H_2O on ternary $Fe_{1-X}X_XAl$ on (110) surface; brown- Fe, light blue- Al, pink representing the adsorbent Pd.

The concentrations were varied from 1 to 4 on each slab since higher concentrations destabilize the systems, leading to brittleness and an increase in oxidation. The most stable slab models with doped concentrations from 1_Pd/Ru up to 4_Pd/Ru were chosen. During the adsorption of H_2O molecules on various ternary $Fe_{1-X}X_XAl$ surfaces, the results show that the lowest adsorption energy was obtained from 2_Pd, followed by 2_Ru and 4_Ru as the least stable, with values of 8.116, 8.234, and 8.305 J m^{-2}, respectively. When the surface coverage was increased up to a monolayer, we noted an increase in E_{ads}/H_2O with increasing coverage for the $Fe_{1-X}X_XAl$ surface, resulting in instability.

Table 1. The adsorption energy of H_2O on the stable site of each ternary $Fe_{1-X}Y_XAl$ system illustrating the surface free energy (SFE), Energy of modified (E_mod) system, energy of Iron (E_Fe), energy of the pristine (E_Prist), energy of the adsorbent (E_X) and adsorption energy (E_{ads}).

Concentration	SFE (J m^{-2})	E_mod (J m^{-2})	E_Fe (J m^{-2})	E_prist (J m^{-2})	E_X (J m^{-2})	E_X/atom (J m^{-2})	E_{ads}/H_2O (J m^{-2})
2_Pd	0.165	-553.663	-4.99	-187.90	-5.21	-1.30	8.116
2_Ru	0.165	-559.174	-4.99	-187.90	-2.72	-1.36	8.234
4_Ru	0.165	-562.499	-4.99	-187.90	-2.72	-1.36	8.305

3.2 O_2 interaction on $Fe_{1-X}Y_XAl$ system

Figures 3 and 4 show how oxygen chemisorbs onto the ternary $Fe_{1-X}Y_XAl$ alloy. It has been demonstrated that O_2 reactions improve surface stability through the formation of an oxide layer (Al_2O_3 [18, 19].

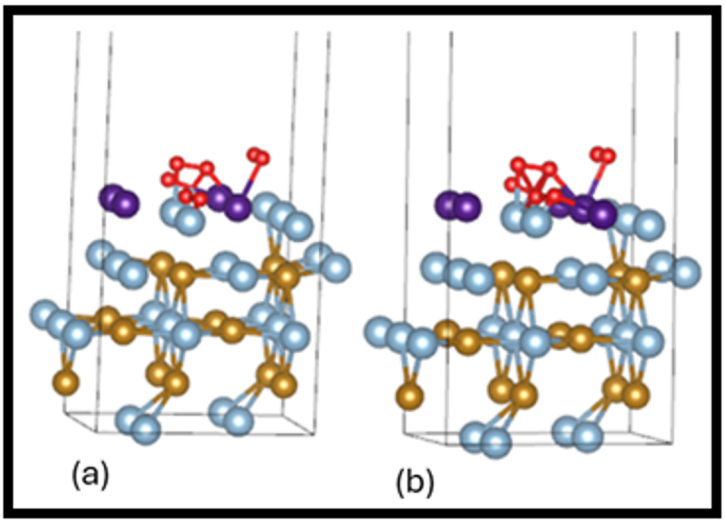

Fig. 3. Adsorption of O_2-bridge on ternary $Fe_{1-X}X_XAl$ on (110) surface; brown- Fe, light blue- Al, dark blue representing the adsorbent Ru.

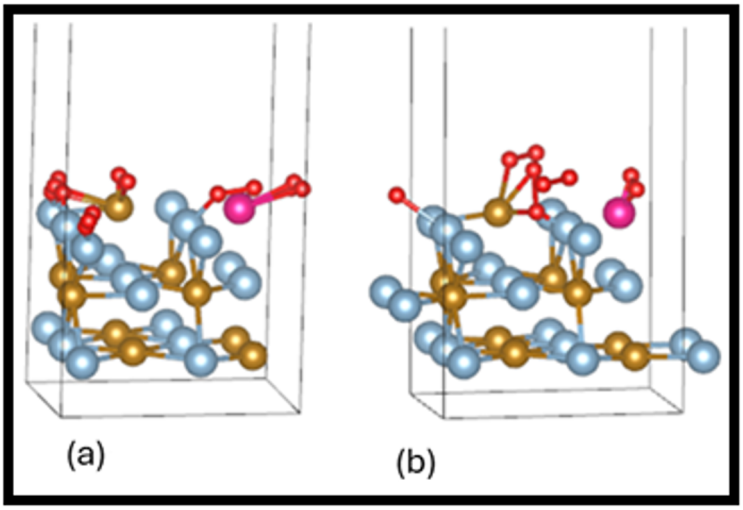

Fig. 4. Adsorption of O_2-mono on ternary $Fe_{1-X}X_XAl$ on (110) surface; brown- Fe, light blue- Al, pink representing the adsorbent Pd.

The O_2 molecule was adsorbed on the ternary $Fe_{1-X}X_XAl$ system as mono and bridge in order to evaluate the surface energies. To obtain accuracy between the nuclei of two bonded atoms. This is based on data from crystal structures of various complexes. The results indicate that 2_Pd_mono had the lowest adsorption energy, followed by 2_Pd_bridge, 4_Ru_mono and 4_Ru_bridge as the least stable with values of 0.794, 0.889, 1.081 and 1.191 J m^{-2}, respectively. When O_2 was adsorbed on the surface of $Fe_{1-X}X_XAl$, the adsorption energy was lower compared to the adsorption of H_2O.

Table 2. Adsorption energy of O_2 on the stable site of each ternary $Fe_{1-X}X_XAl$ system, indicating the surface free energy (SFE), Energy of modified (E_mod) system, energy of Iron (E_Fe), energy of the pristine (E_Prist), energy of the adsorbent (E_X), and the adsorption energy (E_{ads}).

Concentrations	SFE ($J\ m^{-2}$)	E_mod ($J\ m^{-2}$)	E_Fe ($J\ m^{-2}$)	E_prist ($J\ m^{-2}$)	E_X ($J\ m^{-2}$)	E_X/atom ($J\ m^{-2}$)	E_{ads}/O_2 ($J\ m^{-2}$)
2_Pd_Mono	0.165	-213.448	-4.99	-187.90	-5.210	-1.303	0.794
2_Pd_Bridge	0.165	-217.868	-4.99	-187.90	-5.210	-1.303	0.889
4_Ru_Mono	0.165	-226.853	-4.99	-187.90	-2.723	-1.362	1.081
4_Ru_Bridge	0.165	-231.978	-4.99	-187.90	-2.723	-1.362	1.191

4 Conclusion

The interaction of O_2 and H_2O on the $Fe_{1-X}X_XAl$ surface was successfully deduced from surface free energy and adsorption energy calculations using DFT. The behaviour of E_{ads}/H_2O showed higher surface energies compared to those of E_{ads}/O_2, which illustrated that E_{ads}/O_2 is more stable with the lower energies. The oxide layer (Al_2O_3) formed through the interaction of Al and O_2, which increases corrosion resistance necessary regardless of the production processes. The deterioration on the surfaces of metals would result in increased oxidation process, pressing demand for more resources, implying high costs of production. This behaviour leads to chemical occurrence on the surface of the material, in particular, how oxidation affects the durability of the $Fe_{1-X}X_XAl$ system, resulting in corrosion. As the metal reacts with the environment, it causes a redox reaction and the deterioration of steel, which is not visible to the naked eye. Hence, the study of surface stability assisted in determining the best process to identify how a protective oxide layer can be formed for component coating for superior protection. The adsorption of O_2 on the surface of the ternary system contributed to the formation of the oxide layer compared to the adsorption of H_2O.

The calculations were carried out at the Materials Modelling Centre (MMC) of the University of Limpopo and the Centre for High Performance Computing (CHPC) in Cape Town. The authors also thank the National Research Foundation (NRF) for financial support. Advanced Materials Initiative (AMI) and MINTEK are greatly appreciated for their funding support. Thank you to Dr Brian Ramogayana for his assistance with the surface work calculations. The authors confirm that the data supporting the findings of this study are available. Raw data that support the findings of this study are available from the corresponding author.

References

1. A. Fones and G. Hatton, Effects of Platinum Group Metals Doping on stainless steel. Platn. Met. Rev. **58**, 1 (2014).
https://doi.org/10.1595/147106714X676640
2. C. T. Liu, E. P. George, P. J. Maziasz and J. H. Schneibel, Recent advances in B2 iron aluminide alloys: Deformation, fracture and alloy design. Mater. Sci. Eng. A **258,** 1-2 (1998).
https://doi.org/10.1016/S0921-5093(98)00921-6

3. J. Cebulski, D. Pasek, M. Bik, K. Świerczek, P. Jeleń, K. Mroczka, J. Dąbrowa, M. Zajusz, J. Wyrwa and M. Sitarz, In-situ XRD investigations of FeAl intermetallic phase-based alloy oxidation, Corros. Sci. **164,** 108344 (2020).
https://doi.org/10.1016/j.corsci.2019.108344
4. B. M. Mutasa, Defect Structures in Ordered Intermetallics; Grain Boundaries and Surfaces in FeAl, NiAl, CoAl and TiAl, (Blacksburg, Virginia Polytechnic Institute and State University, 1997).
5. P. A. Mc Quay, V. K. Sikka, Y.E. Khalfalla and K.Y. Benyounis, Casting of Intermetallics, Mater. Sci. **6**, 2001 (2016).
doi:10.1016/B0-08-043152-6/00187-X
6. C. S. Mkhonto, N. L. Lethole, P. E. Ngoepe and H. R. Chauke, digital technology in production development, The 23rd Annual International Conference at the Hazendal wine estate in Stellenbosch, RAPDASA Conference, November 8 - 11 (2022).
https://doi.org/10.1051/matecconf/202237009006
7. C. S. Mkhonto, P. E. Ngoepe and H. R. Chauke, in Proceedings of the MRS Advances-2020 conference, materials education/networking in materials science & engineering, Nelson Mandela African Institute for Science and Technology, in Arusha, Tanzania, from December 10 – 13, (2020).
DOI: 10.1557/adv.2020.177
8. C. S. Mkhonto, P. E. Ngoepe and H. R. Chauke, Advanced Manufacturing Beyond Borders, The 24th Annual International Conference, CSIR International Convention Centre in Pretoria, 30 October - 02 November, (2023).
https://doi.org/10.1051/matecconf/202338802004
9. G. Fu, Z. Qi, Y. Su, Q. Liu and X. Guo, Effect of Different Treatment on Corrosion, High Temp. Mater. **33**, 6 (2014).
https://doi.org/10.1515/htmp-2013-0110
10. J. Cebulski, D. Pasek, M. Sozanska, M. Popczyk, J. Gabor and A. Swinarew, "Oxodation of the alloy based on the intermetallic phase FeAl in the temperature range of 700-1000oC in air and posssibilities of practical application, Mater. **18**, 1835 (2025).
https://doi.org/10.3390/ma18081835
11. Y. N. Mansurov and J. U. Rakhmonov, Analysis of the phase composition and the structure of aluminum alloys with increased content of impurities, Mater. Sci. **2** (2018).
DOI: 10.17580/nfm.2018.02.07
12. A.E. Mattson, P.A. Schultz, M.P. Desjarlais, T.R. Mattsson and K. Leung, Designing meaningful density functional theory calculations in materials science, Mod. and Simul. Mater. Sci. Eng. **1** (2005).
DOI 10.1088/0965-0393/13/1/R01
13. J.P. Perdew, K. Burke and M. Ernzerhof, Generalized gradient approximation made simple, Phys. Rev. Lett. **77**, 1396 (1996).
https://doi.org/10.1103/PhysRevLett.77.3865
14. E. Matthias and J.P. Perdew, Generalized gradient approximation to the angle- and system-averaged exchange hole, J. Chem. Phys. **109**, 9 (1998).
https://doi.org/10.1063/1.476928
15. G. Kresse and J. Furthmüller, Efficient iterative schemes for ab initio total-energy calculations using a plane-wave basis set, Phys. Rev. B **54**, 11169 (1996)
https://doi.org/10.1103/PhysRevB.54.11169
16. G. W. Watson, E. T. Kelsey, N. H. de Leeuw, D. J. Harris and S. C. Parker, Faraday Transition Atomistic simulation of dislocations, surfaces and interfaces in MgO, J. Chem. Soc. **92**, 3 (1996).
https://doi.org/10.1039/FT9969200433

17. M. J. Ungerer, D. Santos-Carballal, A. Cadi-Essadek, C. G. C. E. van Sittert, and N. H. de Leeuw, Interaction of H2O with the Platinum Pt (001), (011), and (111) Surfaces: A Density Functional Theory Study with Long-Range Dispersion Corrections, J. Phys. Chem. C **123**, 27466 (2019).
https://doi: 10.1021/acs.jpcc.9b06136
18. P. G. Gonzales-Ormeno, H. M. Petrilli and C. G. Schon, Ab initio calculation of the bcc Fe-Al phase diagram including magnetic interactions, Scripta Mater. **54**, 7 (2006).
https://doi.org/10.1016/j.scriptamat.2005.12.024
19. K. M. Doleker, The Examination of Microstructure and Thermal Oxidation behaviour of laser-remelted high-velocity oxygen liquid fuel Fe/Al coating, J. Mater. Eng. Perfor. **29**, 5 (2020).
https://doi.org/10.1007/s11665-020-04873-z